Journal of Solid State Chemistry 181 (2008) 2370–2377

Contents lists available at ScienceDirect

Journal of Solid State Chemistry

journal homepage: www.elsevier.com/locate/jssc

Solvothermal syntheses, and characterization of $[Ln(en)_4(SbSe_4)]$ (Ln = Ce, Pr) and $[Ln(en)_4]SbSe_4 \cdot 0.5en$ (Ln = Eu, Gd, Er, Tm, Yb): The effect of lanthanide contraction on the crystal structures of lanthanide selenidoantimonates(V)

Dingxian Jia *, Aimei Zhu, Qinyan Jin, Yong Zhang, Wenqing Jiang

School of Chemistry and Chemical Engineering, Suzhou University, Suzhou 215123, PR China

ARTICLE INFO

Article history:
Received 1 April 2008
Received in revised form
24 May 2008
Accepted 30 May 2008
Available online 4 June 2008

Keywords:
Lanthanide
Selenidoantimonates
Antimony
Solvothermal synthesis
Lanthanide contraction

ABSTRACT

Two types of lanthanide selenidoantimonates $[Ln(en)_4(SbSe_4)]$ (Ln = Ce(**1a**), Pr(**1b**)) and $[Ln(en)_4]SbSe_4 \cdot 0.5en$ (Ln = Eu(**2a**), Gd(**2b**), Er(**2c**), Tm(**2d**), Yb(**2e**); en = ethylenediamine) were solvothermally synthesized by reactions of $LnCl_3$, Sb and Se with the stoichiometric ratio in en solvent at 140 °C. The four-en coordinated lanthanide complex cation $[Ln(en)_4]^{3+}$ formed *in situ* balances the charge of $SbSe_4^{3-}$ anion. In compounds **1a** and **1b**, the $SbSe_4^{3-}$ anion act as a monodentate ligand to coordinate complex $[Ln(en)_4]^{3+}$ and the neutral compound $[Ln(en)_4(SbSe_4)]$ is formed. The Ln^{3+} ion has a nine-coordinated environment involving eight N atoms and one Se atom forming a distorted monocapped square antiprism. In **2a–2e** the lanthanide(III) ion exists as isolated complex $[Ln(en)_4]^{3+}$, in which the Ln^{3+} ion is in a bicapped trigonal prism geometry. A systematic investigation of the crystal structures reveals that two types of structural features of these lanthanide selenidoantimonates are related with lanthanides contraction across the lanthanide series. TG curves show that compounds **1a–1b** and **2a–2e** remove their organic components in one and two steps, respectively.

1. Introduction

In the past decade, the mild solvothermal synthesis of Main Group chalcogenometalates containing transition metal (TM) complexes has attracted increasing attention [1–4]. The reactions are usually conducted in amine solutions in the presence of transition metals. The amines act not only as reaction solvents, but also as ligands to coordinate with TM^{n+} forming complex cations ($TM(amine)_m^{n+}$), which act as space fillers and/or charge compensating ions in chalcogenometalate compounds. In the case of chalcogenoantimonates, a series of thioantimonates and selenidoantimonates with various structures depending on the transition metals and amines used, have been prepared by the solvothermal method [5–28]. However, the solvothermal route to synthesis of lanthanide chalcogenometalates remains unexplored. Recently, we started to investigate whether it is possible to prepare thioantimonates containing lanthanide (Ln) metal complexes using the solvothermal method. The integration of lanthanide metals with thioantimonates will alter the component and structures of such thioantimonate compounds, and thus, changes their physical and chemical properties. According to this idea, we successfully synthesized series of thioantimonates containing lanthanide(III)–en complexes in the system Ln/Sb/S/en under the solvothermal conditions [29,30]. A systematic investigation on the crystal structures of these lanthanide thioantimonates shows that the early lanthanide metals (La–Sm) form one-dimensional neutral polymers $[Ln(en)_3(H_2O)_x(\mu_{3-x}\text{-}SbS_4)]_\infty$ ($x = 0$ or 1), in which the SbS_4^{3-} anion act as a tridentate or bidentate ligand to bridge $[Ln(en)_3]^{3+}$ ions. The rest lanthanide metals form compounds with the general formula $[Ln(en)_4]SbS_4 \cdot 0.5en$. The lanthanide(III)–en complexes exhibit dramatically different structure-directing effect compared to the $[TM(en)_3]^{3+}$ cations. In the presence of lanthanide(III)–en complexes, only thioantimonates(V) are obtained, while $[TM(en)_3]^{3+}$ complexes are suitable structure directors for the formation of thioantimonates(III) [5–22,28].

Very recently, we extended the solvothermal method to the Ln/Sb/Se/en system and prepared three new lanthanide selenidoantimonates(V) $[La(en)_4(SbSe_4)]$ (**1c**), $[Nd(en)_4(SbSe_4)]$ (**1d**) and $[Sm(en)_4]SbSe_4 \cdot 0.5en$ (**2f**) [31]. To clarify the relationship between the molecular structure of the lanthanide selenidoantimonates and the entity of the lanthanide(III) series, more lanthanide selenidoantimonate compounds are needed. The present contribution reports the synthesis, crystal structures of seven new members of lanthanide selenidoantimonates(V) $[Ln(en)_4(SbSe_4)]$ (Ln = Ce, Pr) and $[Ln(en)_4]SbSe_4 \cdot 0.5en$ (Ln = Eu, Gd, Er, Tm, Yb), and the influence of lanthanides contraction across the lanthanide series on the crystal structures of these compounds is discussed.

* Corresponding author. Fax: +86 512 65880089.
E-mail address: jiadingxian@suda.edu.cn (D. Jia).

0022-4596/$ - see front matter © 2008 Elsevier Inc. All rights reserved.
doi:10.1016/j.jssc.2008.05.040

2. Experimental section

2.1. Materials and physical measurements

All analytical grade chemicals were obtained commercially and used without further purification. Elemental analysis was conducted on a MOD 1106 elemental analyzer. FT-IR spectra were recorded with a Nicolet Magna-IR 550 spectrometer in dry KBr discs in the 4000–400 cm^{-1} range. Diffuse reflection spectra of the powdered samples were measured on a Shimadzu UV-3150 spectrophotometer at room temperature. The absorption (α/S) data were calculated from the reflectance using the Kubelka–Munk function $\alpha/S = (1-R)^2/2R$ [32], where R is the reflectance at a given energy, α is the absorption, and S is the scattering coefficient. Thermoanalytical measurements was performed using a TG-DSC microanalyzer of SDT 2960 and all the samples were heated under a nitrogen stream of 100 ml min^{-1} with a heating rate of 5 °C min^{-1}.

2.2. Synthesis

All compounds were synthesized in ethylenediamine (en) under the mild solvothermal conditions. In a typical synthetic procedure, reactants in the certain molar ratio were dispersed in en under stirring and then the mixture was loaded into a Teflon-lined stainless steel autoclave with inner volume of 15 ml. The sealed autoclave was heated at 140 °C for 7 days. After cooled to ambient temperature, crystals were filtered off, washed with ethanol and ether and stored under vacuum.

2.2.1. Synthesis of $[Ce(en)_4(SbSe_4)]$ (**1a**)

The red block crystals of **1a** were obtained by the reaction of $CeCl_3$ (123 mg, 0.5 mmol), Sb (61 mg, 0.5 mmol), and Se (158 mg, 2 mmol) in 2 ml en with the yield of about 62% based on Sb. Anal. Found: C 11.65, H 3.88, N 13.64. Calc. for $C_8H_{32}N_8Se_4CeSb$: C 11.74, H 3.94, N 13.70%. IR (KBr): 3382s, 3239s, 3101s, 2928s, 2868m, 1582 vs, 1489s, 1451s, 1388m, 1325s, 1276m, 1146w, 1101w, 1007 vs, 860w, 822w, 633m, 496 m cm^{-1}.

2.2.2. Synthesis of $[Pr(en)_4(SbSe_4)]$ (**1b**)

Yellow block crystals of **1b** were obtained in 72% yield (based on Sb) using the same synthesis procedure as used in **1a** except that reactant $PrCl_3$ was used instead of $CeCl_3$. Anal. Found: C 11.61, H 3.89, N 13.59. Calc. for $C_8H_{32}N_8Se_4PrSb$:C 11.73, H 3.94, N 13.68%. IR (KBr): 3380s, 3236s, 3104s, 2928s, 2868m, 1583s, 1489s, 1453s, 1388m, 1324s, 1276m, 1147w, 1102w, 1005 vs, 860w, 633m, 498 m cm^{-1}.

2.2.3. Synthesis of $[Eu(en)_4]SbSe_4 \cdot 0.5en$ (**2a**)

Orange-red block crystals of **2a** were obtained in 66% yield (based on Sb) using the same synthesis procedure as used in **1a** except that reactant $EuCl_3$ was used instead of $CeCl_3$. Anal. Found: C 12.44, H 4.08, N 14.52. Calc. for $C_9H_{36}N_9Se_4EuSb$: C 12.57, H 4.22, N 14.66%. IR (KBr): 3388s, 3335s, 3241s, 3164s, 2938s, 2869s, 1595s, 1579s, 1481, 1386m, 1354s, 1211w, 1159w, 1078s, 1030 vs, 822w, 779w, 641s, 513 w cm^{-1}.

2.2.4. Synthesis of $[Gd(en)_4]SbSe_4 \cdot 0.5en$ (**2b**)

Orange block crystals of **2b** were obtained in 42% yield (based on Sb) using the same synthesis procedure as used in **1a** except that reactant $GdCl_3$ was used instead of $CeCl_3$. Anal. Found: C 12.25, H 4.84, N 14.35. Calc. for $C_9H_{36}N_9Se_4GdSb$: C 12.49, H 4.91, N 14.57%. IR (KBr): 3382s, 3347s, 3239s, 3101s, 2927s, 2868m, 1582 vs, 1490s, 1451s, 1384m, 1325s, 1276m, 1146w, 1101w, 1007 vs, 860w, 822w, 633m, 588 m cm^{-1}.

2.2.5. Synthesis of $[Er(en)_4]SbSe_4 \cdot 0.5en$ (**2c**)

Orange block crystals of **2c** were obtained in 48% yield (based on Sb) using the same synthesis procedure as used in **1a** except that reactant $ErCl_3$ was used instead of $CeCl_3$. Anal. Found: C 12.27, H 4.07, N 14.29.Calc. for $C_9H_{36}N_9Se_4ErSb$: C 12.35, H 4.14, N 14.40%. IR (KBr): 3303 vs, 3282s, 3245s, 3132s, 2930 vs, 2882s, 1570 vs, 1511s, 1386m, 1331s, 1154w, 1007s, 866w, 814w, 776w, 662w, 496 m cm^{-1}.

2.2.6. Synthesis of $[Tm(en)_4]SbSe_4 \cdot 0.5en$ (**2d**)

Red block crystals of **2d** were obtained in 48% yield (based on Sb) using the same synthesis procedure as used in **1a** except that reactant $TmCl_3$ was used instead of $CeCl_3$. Anal. Found: C 12.06, H 4.03, N 14.24. Calc. for $C_9H_{36}N_9Se_4TmSb$ (876.99): Calcd. C 12.35, H 4.14, N 14.40; found: C 12.27, H 4.07, N 14.31. IR (KBr): 3303 vs, 3245s, 3172s, 2910s, 2863s, 1582 vs, 1511s, 1386m, 1331s, 1154w, 1007s, 872w, 826w, 775w, 548 m cm^{-1}.

Table 1
Crystallographic data for **1a–2e**

	1a	1b	2a
Formula	$C_8H_{32}N_8Se_4CeSb$	$C_8H_{32}N_8Se_4PrSb$	$C_9H_{36}N_9Se_4EuSb$
Formula mass	818.13	818.92	860.02
Crystal system	Monoclinic	Monoclinic	Monoclinic
Space group	$P2_1/n$	$P2_1/n$	$P2_1/n$
a (Å)	9.4644(14)	9.4699(14)	11.3379(19)
b (Å)	14.676(2)	14.625(2)	13.104(2)
c (Å)	16.018(2)	15.943(2)	16.328(3)
β (°)	98.900(3)	98.898(3)	92.543(3)
V (Å^3)	2198.2(6)	2181.5(5)	2423.5(7)
Z	4	4	4
T (K)	193(2)	153(2)	153(2)
Dcalc (g cm^{-3})	2.472	2.493	2.357
F (000)	1524	1528	1612
μ (mm^{-1})	9.904	9.568	9.699
Measured reflections	21142	20858	23210
Independent reflections	4020	3984	4432
R_{int}	0.0494	0.0829	0.0346
Reflections with ($I > 2\sigma(I)$)	3702	3357	4188
Parameters	200	200	225
R_1	0.0349	0.0377	0.0282
wR_2	0.0697	0.0798	0.0561
Goodness-of-fit on F^2	1.182	1.010	1.177

2b	2c	2d	2e
$C_9H_{36}N_9Se_4GdSb$	$C_9H_{36}N_9Se_4ErSb$	$C_9H_{36}N_9Se_4TmSb$	$C_9H_{36}N_9Se_4YbSb$
865.31	875.32	876.99	881.10
Monoclinic	Monoclinic	Monoclinic	Monoclinic
$P2_1/n$	$P2_1/n$	$P2_1/n$	$P2_1/n$
11.3795(16)	11.3499(15)	11.395(2)	11.3437(13)
13.1254(17)	13.1254(16)	13.133(2)	13.1254(15)
16.323(2)	16.222(2)	16.227(3)	16.1784(19)
92.453(4)	92.609(3)	92.395(5)	92.696(3)
2435.7(6)	2414.1(5)	2426.3(8)	2406.1(5)
4	4	4	4
223(2)	193(2)	295(2)	193(2)
2.360	2.408	2.401	2.432
1616	1632	1636	1640
9.798	10.615	10.759	11.049
23408	23132	22991	22983
4449	4412	4431	4397
0.0582	0.0451	0.0660	0.0408
3877	4017	4075	4044
225	225	232	225
0.0441	0.0366	0.0406	0.0340
0.0854	0.0742	0.0899	0.0647
1.164	1.167	1.149	1.162

*2.2.7. Synthesis of [Yb(en)$_4$]SbSe$_4$ · 0.5en (**2e**)*

Red block crystals of **2e** were obtained in 68% yield (based on Sb) using the same synthesis procedure as used in **1a** except that reactant $YbCl_3$ was used instead of $CeCl_3$. Anal. Found: C 12.06, H 4.03, N 14.24. Calc. for $C_9H_{36}N_9Se_4YbSb$: C 12.27, H 4.12, N 14.31%. IR (KBr): 3301 vs, 3282s, 3245s, 3132s, 2928 vs, 2881s, 1570vs, 1515s, 1385m, 1331s, 1156w, 1007s, 868w, 814w, 664w, 495 m cm^{-1}.

2.3. X-ray crystallography

Data were collected on a Rigaku Mercury CCD diffractometer using graphite-monochromated Mo-$K\alpha$ radiation ($\lambda = 0.71073$ Å) with a ω-scan method to a maximum 2θ value of 50.70°. An absorption correction was applied for all the compounds using multi-scan. The structures were solved with direct methods using the program of SHELXS-97 [33]. The refinement was performed against F^2 using SHELXL-97 [34]. All the non-hydrogen atoms were refined anisotropically. The atoms C(8) in **2a**, **2b**, **2d** and **2e**, and C(7) in **2c** are disordered, and the occupancies of the disordered atoms are assigned as 52% and 48%, 58% and 42%, 55% and 45%, 40% and 60%, and 54% and 46% for **2a**, **2b**, **2c**, **2d**, and **2e**, respectively. The hydrogen atoms were positioned with idealized geometry and refined with fixed isotropic displacement parameters. Technical details of data collections and refinement are summarized in Table 1.

3. Results and discussion

3.1. Structures of *1a* and *1b*

Compounds **1a** and **1b** crystallize in space group $P2_1/n$ of the monoclinic system with two formula units and are isostructural with **1c** and **1d**. The molecular structure of **1a** is depicted in Fig. 1. The Ce^{3+} ion is coordinated by four bidentate en ligands and a monodentate $SbSe_4^{3-}$ forming the neutral complex [Ce(en)$_4$(SbSe$_4$)]. The cerium center lies within a nine-coordinated environment forming the polyhedron CeN_8Se, which can be described as a distorted monocapped square antiprism with atoms N1, N6, Se1, and N8 forming one face, and N2, N3, N4, and N5 forming the opposite face. The capping position is occupied by atom N7. The *Ln*–N bond lengths 2.646(5)–2.768(5) Å for Ce–N (av. 2.702(5) Å), 2.587(5)–2.728(5) Å for Pr–N (av. 2.650(5) Å) (Table 2) are consistent with those of reported cerium(III)- and praseodymium(III)–en complexes, respectively [35,36]. The Ce–Se (3.3163(7) Å) and Pr–Se (3.2985(8) Å) bond lengths in *Ln*N$_8$Se polyhedron are longer than those observed in seven- or six-coordinated lanthanide complexes, such as the bond lengths 2.9633(7)–3.1975(7) Å for Ce–Se of $CeSe_6$ polyhedron in $CeCuSe_2$ [37], 3.0179(9)–3.2830(9) Å for Ce–Se of $CeOSe_6$ polyhedron in Ce_4MnOSe_6 [38] and Ce_4FeOSe_6 [38], 2.947(1)–3.180(1) Å for Pr–Se of $PrSe_6$ polyhedron in $PrCuSe_2$ [37]. The *Ln*–N and *Ln*–Se lengths decrease with the radius decrease from Ce to Pr.

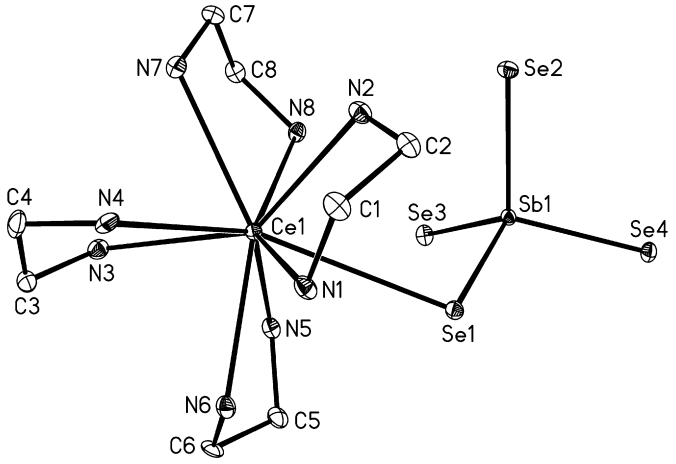

Fig. 1. Crystal structure of **1a** with the labeling scheme (30% thermal ellipsoids). Hydrogen atoms are omitted for clarity.

Table 2
Selected bond distances (Å) and angles (°) for **1a** and **1b**

	1a (*Ln* = Ce)	**1b** (*Ln* = Pr)
Sb–Se	2.4660(7)–2.4693(8)	2.4648(8)–2.4697(8)
Ln–Se	3.3163(7)	3.2985(8)
Ln–N	2.646(5)–2.768(5)	2.587(5)–2.728(5)
Se–Sb–Se	107.70(3)–111.53(3)	107.64(3)–111.63(3)
Sb–Se–*Ln*	102.95(2)	103.92(3)
Se–*Ln*–N	69.52(11)–141.18(11)	68.89(12)–141.11(13)
N–*Ln*–N	62.63(15)–145.40(15)	63.51(16)–144.75(16)

The tetraselenidoantimonate anion $SbSe_4^{3-}$ acts as a monodentate ligand to coordinate with $[Ln(en)_4]^{3+}$ complex via the atom Se(1). Because the Se(1) atom bridges lanthanide(III) and antimony(V) centers, the Sb(1)–Se(1) bond length (2.4816(8) Å for **1a**, 2.4826(9) Å for **1b**) is expectedly longer than the rest three Sb–Se bonds (Table 2). The $SbSe_4^{3-}$ anion can be described as a distorted tetrahedron, as evidenced by the Se–Sb–Se angles ranging from 107.70(3)° to 111.53(3)° for **1a**, and 107.64(3)–111.63(3)° for **1b** (Table 2). Both bond lengths and angles are comparable to those observed in other compounds containing $SbSe_4^{3-}$ tetrahedral anion [24,25]. The $SbSe_4^{3-}$ anion acting as ligands to transition metal centers has been observed in compounds $[Mn(en)_3]_2[Mn_4(en)_9(SbSe_4)_4]$ [24], $[Mn(en)_3][Mn_2(SbSe_4)_2(en)_4(H_2O)]$ [27], and $[Mn(en)_3][Mn_2(en)_4(H_2O)_2(\mu\text{-}SbSe_4)][Mn(\mu\text{-}SbSe_4)(en)_2]Cl_2$ [27]. To the best of our knowledge, the compounds **1a**–**1d** are the only examples of selenidoantimonate(V) compounds in which the $SbSe_4^{3-}$ anion acts as ligands to lanthanide(III) centers in amine solutions.

In **1a**, the Se(1) and Se(4) atoms of $SbSe_4^{3-}$ anion are involved in hydrogen bond formation with the $-NH_2$ groups of two adjacent molecules, leading to a layered arrangement (Fig. 2) of [Ce(en)$_4$(SbSe$_4$)] molecules parallel to the (101) plane of unit cell (Fig. 3). The layers are further connected through N–H···Se hydrogen bonds leading to a three-dimensional network (Fig. 3). The interlayer hydrogen bonds are formed by Se(2) and Se(3) atoms with $-NH_2$ groups. The N···Se lengths vary from 3.440(5) to 3.878(5) Å and N–H···Se angles vary from 138.6° to 170.6° (Table 3). The similar intermolecular hydrogen bond interactions are observed in compound **1b** (Table 3).

3.2. Structures of *2a*–*2e*

Compounds **2a**–**2e**, with the general formula $[Ln(en)_4]SbSe_4 \cdot 0.5en$ (*Ln* = Eu(**2a**), Gd(**2b**), Er(**2c**), Tm(**2d**), Yb(**2e**)), crystallize in the monoclinic space group $P2_1/n$ with four formulae units in the unit cell and are isostructural. They consist of an isolated four-en coordinated lanthanide complex cation $[Ln(en)_4]^{3+}$ (*Ln* = Eu, Gd, Er, Tm, Yb), a tetrahedral anion $SbSe_4^{3-}$, and a free en molecule. The crystal structure of **2a** is depicted in Fig. 4. The atom C(8) is disordered with the occupancies of 52% and 48%. The Ln^{3+} ion is in an eight-coordinated environment with eight amino N atoms from four en ligands forming a distorted bicapped trigonal prism. The *Ln*–N bond lengths are 2.522(4)–2.594(4) Å for Eu–N (av. 2.549(4) Å), 2.503(6)–2.571(7) Å for Gd–N

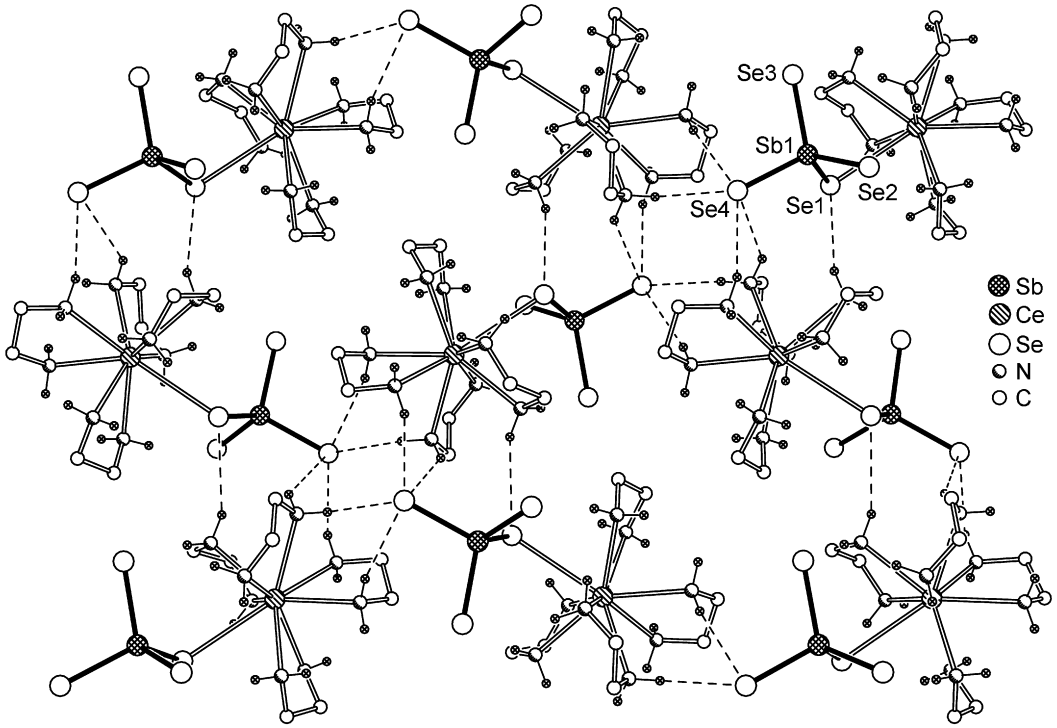

Fig. 2. Section of the crystal packing of **1a** showing N–H···Se intermolecular interactions. Hydrogen atoms of CH_2 are omitted for clarity.

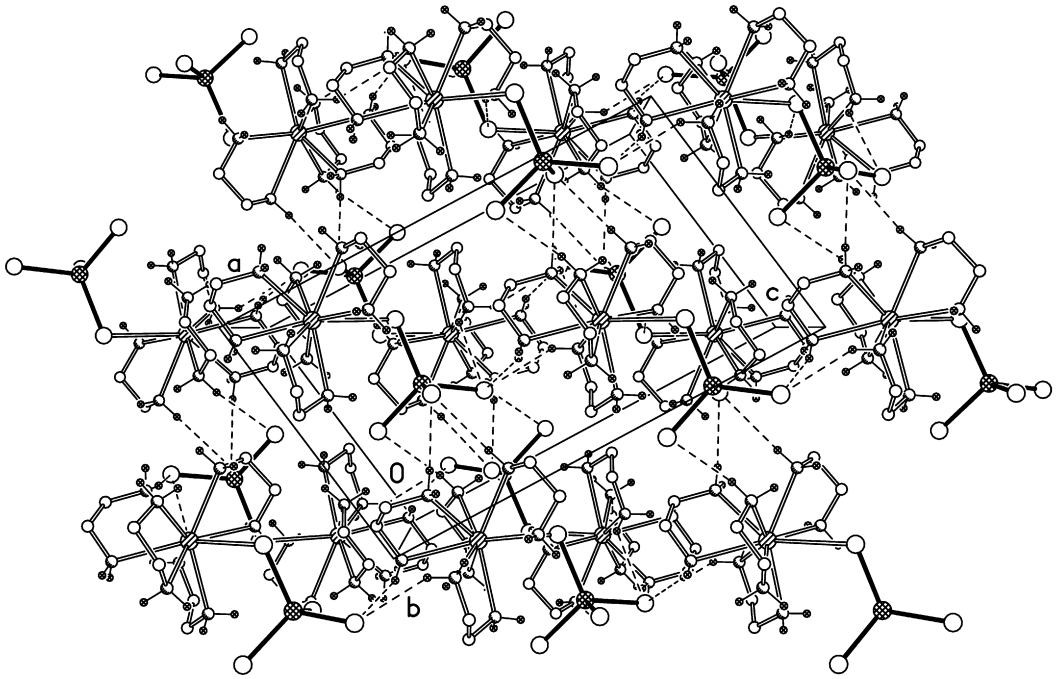

Fig. 3. The crystal packing of **1a** viewed along *b*-axis. Hydrogen atoms of CH_2 are omitted for clarity.

(av. 2.540(6) Å), 2.455(5)–2.520(6) Å for Er–N (av. 2.491(5) Å), 2.445(6)–2.518(6) Å for Tm–N (av. 2.487(6) Å), and 2.426(5)–2.496(5) Å for Yb–N (av. 2.467(5) Å) (Table 4), and are consistent with those observed in other lanthanide complexes with amino donor atoms, respectively [30,39,40]. The *Ln*–N lengths of compounds **1a**, **1b**, and **2a**–**2e** decrease from Ce to Yb because of the lanthanides contraction effect across the lanthanide series. The Sb–Se distances and Se–Sb–Se angles (Table 4) are in good agreement with those found in isolated $SbSe_4^{3-}$ anions [23,41]. Extensive intermolecular hydrogen bond interactions are found in compounds **2a**–**2e**. All Se atoms of the $SbSe_4^{3-}$ anion are involved hydrogen bonding with the $-NH_2$ groups of en ligands. In compound **2a**, each of the $SbSe_4^{3-}$ anions contacts with four $[Eu(en)_4]^{3+}$ cations and two free en molecules, forming thirteen N–H···Se hydrogen bonds with N···Se lengths ranging from 3.390(4) to 3.786(4) Å and N–H···Se angles ranging from 138.6° to 171.1° (Fig. 5). Between the free en molecule and en ligand, hydrogen bond N(4)–H(4B)···N(9) is observed with N(4)···N(9)

Table 3
Hydrogen bond distances (Å) and angles (°) for **1a** and **1b**

D–H···A	d(H···A)	d(D···A)	<(DHA)
1			
N(1)–H(1A)···Se(4)[a]	2.78	3.653(5)	159.6
N(2)–H(2A)···Se(2)[b]	2.61	3.440(5)	149.8
N(2)–H(2B)···Se(4)[c]	2.61	3.498(5)	161.6
N(3)–H(3A)···Se(2)[b]	2.90	3.757(5)	156.0
N(4)–H(4A)···Se(2)	2.71	3.619(5)	170.6
N(4)–H(4B)···Se(1)[c]	3.02	3.878(5)	155.5
N(5)–H(5A)···Se(4)[a]	2.83	3.642(5)	148.0
N(5)–H(5B)···Se(4)[c]	3.03	3.768(5)	138.6
N(6)–H(6A)···Se(2)	2.69	3.583(5)	163.5
N(6)–H(6B)···Se(3)	2.73	3.484(5)	139.4
N(7)–H(7B)···Se(3)	2.69	3.593(5)	167.4
N(8)–H(8B)···Se(3)[b]	2.73	3.547(5)	148.9
2			
N(1)–H(1B)···Se(2)[b]	2.94	3.785(6)	154.3
N(2)–H(2A)···Se(1)[d]	3.03	3.886(5)	156.5
N(2)–H(2B)···Se(2)	2.71	3.620(6)	173.3
N(3)–H(3A)···Se(4)[d]	3.02	3.775(6)	140.9
N(3)–H(3B)···Se(4)[a]	2.80	3.616(6)	149.2
N(4)–H(4A)···Se(3)	2.73	3.475(5)	139.5
N(4)–H(4B)···Se(2)	2.70	3.587(5)	166.3
N(5)–H(5A)···Se(3)	2.70	3.588(5)	166.8
N(6)–H(6A)···Se(3)[b]	2.75	3.557(5)	148.3
N(7)–H(7B)···Se(4)[a]	2.79	3.653(6)	158.4
N(8)–H(8A)···Se(4)[d]	2.63	3.497(5)	160.1
N(8)–H(8B)···Se(2)[b]	2.62	3.434(6)	148.8

Symmetry transformations used to generate equivalent atoms: [a] $x-1/2, -y+1/2, z+1/2$; [b] $x-1, y, z$; [c] $-x+1/2, y-1/2, -z+3/2$; [d] $-x+1/2, y+1/2, -z+3/2$.

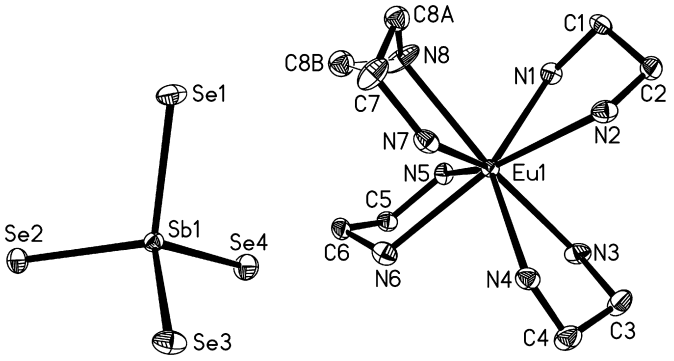

Fig. 4. Crystal structure of **2a** with the labeling scheme (50% thermal ellipsoids). Hydrogen atoms and free en molecule are omitted for clarity.

Table 4
Selected bond distances (Å) and angles (°) for **2a–2e**

	2a (*Ln* = Eu)	**2b** (*Ln* = Gd)	**2c** (*Ln* = Er)
Sb–Se	2.4534(6)–2.4791(6)	2.4540(9)–2.4787(9)	2.4520(8)–2.4795(8)
Ln–N	2.522(4)–2.594(4)	2.503(6)–2.571(7)	2.455(5)–2.520(6)
Se–Sb–Se	105.19(2)–113.89(2)	105.29(3)–113.90(3)	104.99(3)–114.16(3)
N–*Ln*–N	66.21(13)–153.93(13)	67.17(2)–153.2(2)	68.14(18)–152.63(17)
	2d (*Ln* = Tm)	**2e** (*Ln* = Yb)	
Sb–Se	2.4499(10)–2.4775(9)	2.4530(8)–2.4798(7)	
Ln–N	2.445(6)–2.518(6)	2.426(5)–2.496(5)	
Se–Sb–Se	105.13(3)–114.14(4)	104.89(3)–114.25(3)	
N–*Ln*–N	67.2(2)–152.5(2)	68.41(17)–152.18(17)	

distance of 3.084(6) and N(6)–H(4B)···N(9) angle of 156.1°. The N–H···Se and N–H···N hydrogen-bonding interactions lead to a three-dimensional network structure of **2a** (Fig. 6). The similar

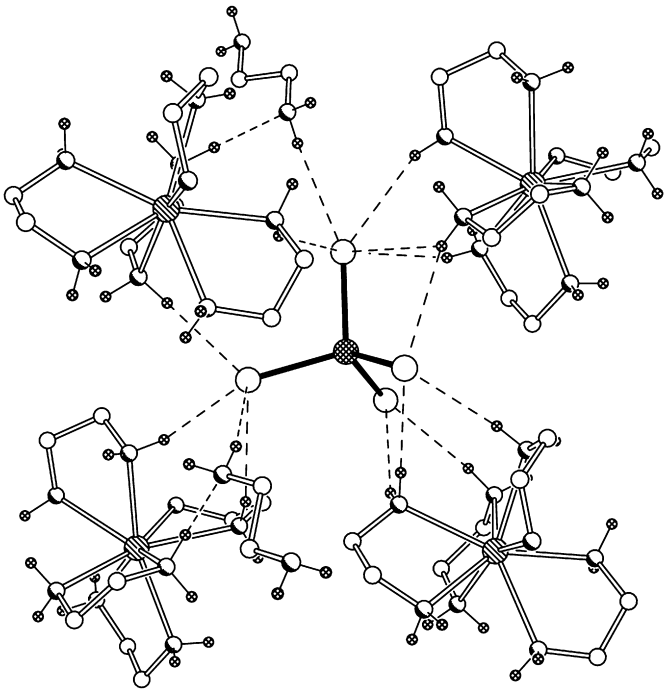

Fig. 5. Section of the crystal packing of **2a** showing the N–H···Se and N–H···N hydrogen bonding. The hydrogen atoms of CH_2 are omitted for clarity.

intermolecular hydrogen bond interactions are observed in compounds **2b–2e**.

3.3. Structural change across the lanthanide series

In our previous work, the reactions of $LaCl_3$ and $NdCl_3$ with Sb and Se in superheated en give isostructural compounds $[La(en)_4(SbSe_4)]$ (**1c**) and $[Nd(en)_4(SbSe_4)]$ (**1d**) respectively, while $SmCl_3$ produces compound $[Sm(en)_4]SbSe_4 \cdot 0.5en$ (**2f**) [31]. Summarizing crystal structures of the compounds **1a–1d** and **2a–2f**, the lanthanide(III) ions form two types of compounds with $SbSe_4^{3-}$ anion in Sb/Se/en system under the identical synthetic conditions. From La to Nd, the lanthanide ion is coordinated by four bidentate en ligands and one monodentate $SbSe_4^{3-}$ anion-forming neutral complexes with the general formula $[Ln(en)_4(SbSe_4)]$ (**1a–1d**). From Sm^{3+} ion, e.g., Sm^{3+}, Eu^{3+}, Gd^{3+}, Er^{3+}, Tm^{3+}, Yb^{3+}, the lanthanide ion existing as an isolated complex cation $[Ln(en)_4]^{3+}$ to balance $SbSe_4^{3-}$ anion leading to the formation of thioantimonate(V) compounds with the general formula $[Ln(en)_4]SbSe_4 \cdot 0.5en$ (**2a–2f**). As a consequence of these results, the dividing point of two types of structures locates between neodymium and samarium. This structural change across the lanthanide series is related with lanthanides contraction. The coordination number of lanthanide(III) ions decreases across the lanthanide series with the decrease in the ionic radius of the trivalent lanthanide ions caused by lanthanides contraction. It is commonly observed that the lighter lanthanide ions prefer coordination number of nine and heavier ones prefer eight in solution [42]. So the four-en coordinated lanthanide $[Ln(en)_4]^{3+}$ complexes leave one coordination site free at the Ln^{3+} ions for lighter lanthanide ions (La^{3+}–Nd^{3+}), enabling bond formation to $SbSe_4^{3-}$ anion, and thus $[Ln(en)_4(SbSe_4)]$ type compounds are formed. However, four bidentate en ligands have saturated the coordination number of heavier lanthanide(III) ions, $SbSe_4^{3-}$ anion has less opportunity to coordinate to the metal center and compounds of type $[Ln(en)_4]SbSe_4 \cdot 0.5en$ (**2a–2f**) are formed.

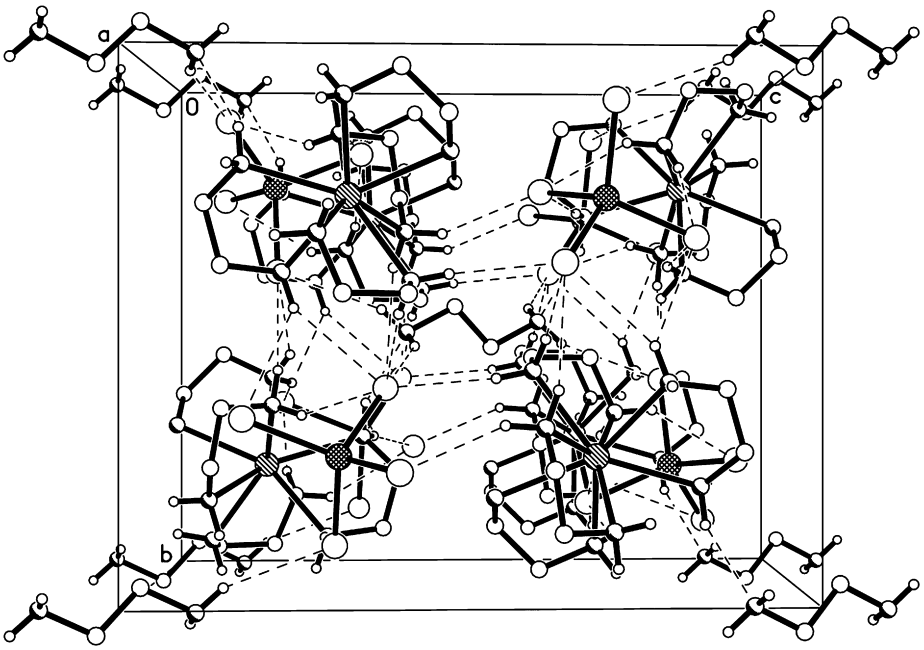

Fig. 6. The crystal packing of **2a** viewed along *a*-axis. Hydrogen atoms of CH_2 are omitted for clarity.

The similar influence of lanthanides contraction effect on crystal structures is observed in the case of lanthanide thioantimonate(V) series [29,30]. We note that SbS_4^{3-} and $SbSe_4^{3-}$ anions exhibit different coordination mode to the lanthanide(III)–en complex ions because of the coordination ability difference between two anions. The SbS_4^{3-} anion can act as a bidentate or tridentate ligand to bridge lighter lanthanide(III) complex $[Ln(en)_3]^{3+}$ cations forming polymers $[Ln(en)_3(H_2O)_x(\mu_{3-x}\text{-}SbS_4)]_\infty$ ($x = 0$ or 1) [29,30], while $SbSe_4^{3-}$ coordinates to lighter lanthanide(III) complex $[Ln(en)_4]^{3+}$ ion as a monodentate ligand forming compounds $[Ln(en)_4(SbSe_4)]$ (**1a**–**1d**). It should be noted that $SbSe_4^{3-}$ anion can act as a bidentate ligand to bridge transition metal complexes, such as $[Mn(en)_2(\mu\text{-}SbSe_4)]^-$ and $[\{Mn(en)_2(H_2O)\}_2(\mu\text{-}SbSe_4)]^+$ fragments in compound $[Mn(en)_3][Mn_2(en)_4(H_2O)_2(\mu\text{-}SbSe_4)][Mn(en)_2(\mu\text{-}SbSe_4)]Cl_2$ [27]. In addition, the coordination mode of $SbSe_4^{3-}$ is also different from that of analogous anion $AsSe_4^{3-}$. The $AsSe_4^{3-}$ anion acts as a μ_3-$AsSe_4$ ligand to bridge $[Ln(dien)_2]^{3+}$ (dien = diethylenetriamine) fragments forming neutral coordination polymers $[Ln(dien)_2(\mu_3\text{-}AsSe_4)]_\infty$ (Ln = Nd, Sm) [43].

3.4. Optical properties

The optical absorption spectra of compounds **1a** and **1b** in the range of 1.7–5.5 eV show well-defined abrupt absorption edges from which the band gaps can be estimated 2.13 eV for **1a**, and 2.27 eV for **1b** (Fig. 7). Both band gaps are larger than those of layered selenidoantimonate(III) compounds $Cu_2SbSe_3 \cdot 0.5en$ (1.58 eV) [26], and Cu_2SbSe_3 en (1.61 eV) [26].

3.5. Thermal analysis

The thermal behaviors of compounds **1a–2e** are investigated under the nitrogen atmosphere, and representative thermalgravimetric curves of **1a** and **2a** are shown in Fig. 8. Compounds **1a** and **1b** get rid of en ligands in a single step with mass losses of 29.0% for **1a** (Fig. 8a) and 28.7% for **1b** between the temperature 200 and 300 °C. The mass losses are in good accordance with the complete removal of eight en ligands (theoretical values: 29.40% for **1a**, 29.36% for **1b**). The decomposition is accompanied by a endothermic event in the DSC curve with the peak temperatures 225 °C (**1a**) and 228 °C (**1b**). Compounds **2a**–**2e** show different decomposition processes from those of compounds **1a** and **1b**. They decompose in two distinct steps with total mass losses of 31.0% (Fig. 8b), 30.5%, 30.2%, 30.1%, and 30.3% for **2a**, **2b**, **2c**, **2d**, and **2e**, respectively. The two-step decomposition is attributed to the loss of the free en molecule between the temperature 90 and 120 °C and the loss of coordinated en ligands between the temperature 200 and 300 °C.

4. Conclusion

Different from the traditional flux method to prepare lanthanide chalcogenides at high temperature, we have successfully synthesized a series of lanthanide(III) selenidoantimonates(V) from the synthetic system *Ln*/Sb/Se/en using the mild solvothermal method. The crystal structures of these selenidoantimonates are influenced by lanthanides contraction effect across the lanthanide series. The early lanthanides, i.e., La–Nd, with their larger ionic radii, form compounds of type $[Ln(en)_4(SbSe_4)]$, in which the four-en coordinated lanthanide complexes $[Ln(en)_4]^{3+}$ are coordinated by the monodentate $SbSe_4^{3-}$ anion. But the heavier lanthanides (Sm–Lu), with their shorter ionic radii because of lanthanides contraction, form compounds of type $[Ln(en)_4]SbSe_4 \cdot 0.5en$, in which the four-en coordinated complexes $[Ln(en)_4]^{3+}$ exist as isolated cations. The synthesis and systematic investigation on the crystal structures of lanthanide selenidoantimonates described in this article will accumulate experience for the designation and preparation of new lanthanide chalcogenometalates by the mild solvothermal method.

Supplementary material

Crystallographic data for the structures reported in this paper have been deposited with the Cambridge Crystallographic Data

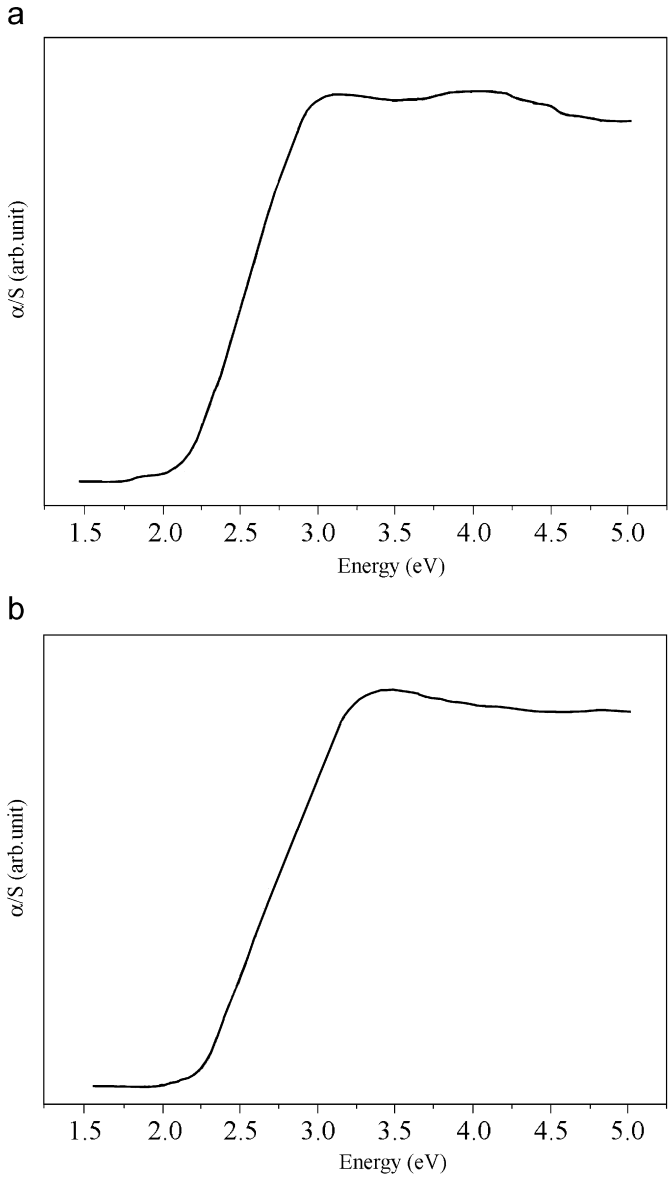

Fig. 7. Optical absorption spectra of **1a** (a) and **1b** (b).

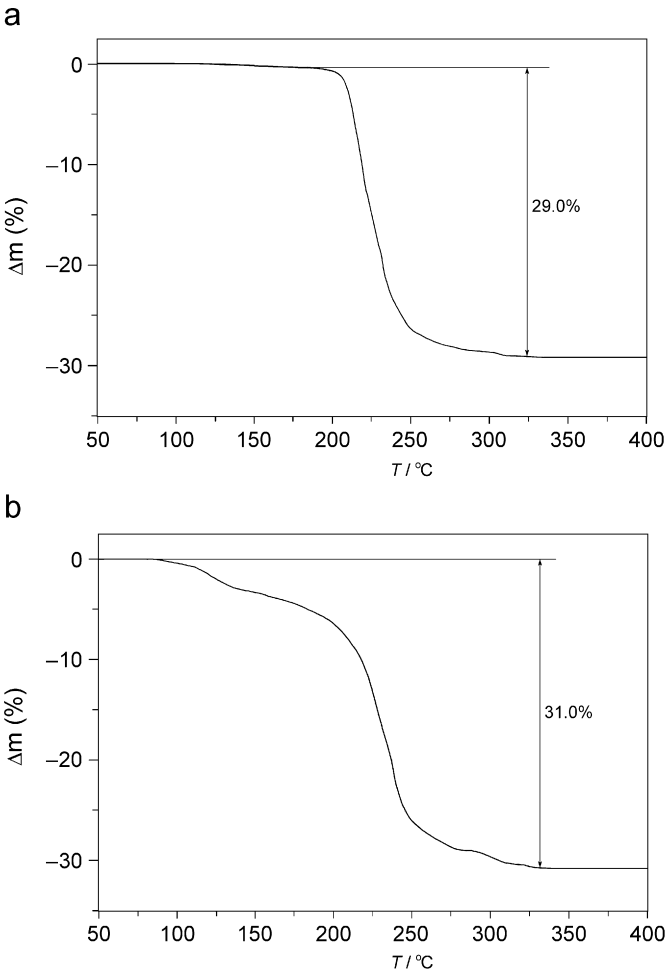

Fig. 8. TG curves of compounds **1a** (a) and **2a** (b).

Centre as supplementary publication number no. CCDC 671145 (**1a**), 671146 (**1b**), 671147 (**2a**), 672103(**2b**), 671148 (**2c**), 672104 (**2d**), and 671149 (**2e**) Copies of the data can be obtained free of charge on application to CCDC, 12 Union Road, Cambridge CB2 1EZ, UK (fax: (+44) 1223 336-033; or e-mail: deposit@ccdc.cam.ac.uk).

Acknowledgments

This work was supported by the National Natural Science Foundation of PR China (No. 20771077), and the Key Laboratory of Organic Synthesis of Jiangsu Province, Suzhou University.

Appendix A. Supplementary Materials

Supplementary data associated with this article can be found in the online version at doi:10.1016/j.jssc.2008.05.040.

References

[1] J. Li, Z. Chen, R.J. Wang, D.M. Proserpio, Coord. Chem. Rev. 190–192 (1999) 707–735.
[2] W.S. Sheldrick, M. Wachhold, Coord. Chem. Rev. 176 (1998) 211–322.
[3] W.S. Sheldrick, J. Chem. Soc. Dalton Trans. (2000) 3041–3052.
[4] S. Dehnen, M. Melullis, Coord. Chem. Rev. 251 (2007) 1259–1280.
[5] H.O. Stephan, M.G. Kanatzidis, J. Am. Chem. Soc. 118 (1996) 12226–12227.
[6] H.O. Stephan, M.G. Kanatzidis, Inorg. Chem. 36 (1997) 6050–6057.
[7] W. Bensch, M. Schur, Z. Naturforsch. 52B (1997) 405–409.
[8] M. Schur, W. Bensch, Z. Naturforsch. 57B (2002) 1–7.
[9] P. Vaqueiro, A.M. Chippindale, A.V. Powell, Inorg. Chem. 43 (2004) 7963–7965.
[10] D.X. Jia, Y. Zhang, J. Dai, Q.Y. Zhu, X.M. Gu, J. Solid State Chem. 177 (2004) 2477–2483.
[11] W. Bensch, C. Näther, R. Stähler, Chem. Commun. (2001) 477–478.
[12] R. Stähler, C. Näther, W. Bensch, Eur. J. Inorg. Chem. (2001) 1835–1840.
[13] R. Stähler, B.-D. Mosel, H. Eckert, W. Bensch, Angew. Chem. Int. Ed. 41 (2002) 4487–4489.
[14] R. Stähler, W. Bensch, Z. Anorg. Allg. Chem. 628 (2002) 1657–1662.
[15] R. Kiebach, W. Bensch, R.-D. Hoffmann, R. Pöttgen, Z. Anorg. Allg. Chem. 629 (2003) 532–538.
[16] P. Vaqueiro, D.P. Darlow, A.V. Powell, A.M. Chippindale, Solid State Ionics 172 (2004) 601–605.
[17] G.L. Schimek, W.T. Pennington, P.T. Wood, J.W. Kolis, J. Solid State Chem. 123 (1996) 277–284.
[18] R. Stähler, W. Bensch, Eur. J. Inorg. Chem. (2001) 3073–3078.
[19] M. Schaefer, R. Stähler, W.-R. Kiebach, C. Näther, W. Bensch, Z. Anorg. Allg. Chem. 630 (2004) 1816–1822.
[20] R. Stähler, W. Bensch, J. Chem. Soc. Dalton Trans. (2001) 2518–2522.
[21] A.V. Powell, S. Boissiere, A.M. Chippindale, J. Chem. Soc. Dalton Trans. (2000) 4192–4195.
[22] M. Schaefer, C. Näther, N. Lehnert, W. Bensch, Inorg. Chem. 43 (2004) 2914–2921.

[23] M.A. Pell, J.A. Ibers, Inorg. Chem. 35 (1996) 4559–4562.
[24] W. Bensch, C. Näther, M. Schur, Chem. Commun. (1997) 1773–1774.
[25] F. Wendland, C. Nather, M. Schur, W. Bensch, Acta Crystallogr. C 54 (1998) 317–319.
[26] Z. Chen, R.E. Dilks, R.J. Wang, J.Y. Lu, J. Li, Chem. Mater. 10 (1998) 3184–3188.
[27] T. van Almsick, W.S. Sheldrick, Z. Anorg. Allg. Chem. 632 (2006) 1413–1415.
[28] D.X. Jia, Y. Zhang, Q.X. Zhao, J. Deng, Inorg. Chem. 45 (2006) 9812–9817.
[29] D.X. Jia, Q.Y. Zhu, J. Dai, W. Lu, W.J. Guo, Inorg. Chem. 44 (2005) 819–821.
[30] D.X. Jia, Q.X. Zhao, Y. Zhang, J. Dai, J.L. Zou, Inorg. Chem. 44 (2005) 8861–8867.
[31] D.X. Jia, Q.X. Zhao, Y. Zhang, J. Dai, J. Zhou, Eur. J. Inorg. Chem. (2006) 2760–2765.
[32] W.W. Wendlandt, H.G. Hecht, Reflectance Spectroscopy, Interscience Publishers, New York, 1966.
[33] G.M. Sheldrick, SHELXS-97, Program for Crystal Structure Determination, University of Göttingen, Germany, 1997.
[34] G.M. Sheldrick, SHELXL-97, Program for the Refinement of Crystal Structures, University of Göttingen, Germany, 1997.
[35] K. Muller-Buschbaum, C.C. Quitmann, Inorg. Chem. 45 (2006) 2678–2687.
[36] D.X. Jia, J. Deng, Q.X. Zhao, Y. Zhang, J. Mol. Struct. 833 (2007) 114–120.
[37] I. Ijjaali, K. Mitchell, J.A. Ibers, J. Solid State Chem. 177 (2004) 760–764.
[38] I. Ijjaali, B. Deng, J.A. Ibers, J. Solid State Chem. 178 (2005) 1503–1507.
[39] R.S. Dickins, S. Aime, A.S. Batsanov, A. Beeby, M. Botta, J.I. Bruce, J.A.K. Howard, C.S. Love, D. Parker, R.D. Peacock, H. Puschmann, J. Am. Chem. Soc. 124 (2002) 12697–12705.
[40] D.X. Jia, A.M. Zhu, J. Deng, Y. Zhang, Z. Anorg. Allg. Chem. 633 (2007) 1246–1250.
[41] M. Wachhold, W.S. Sheldrick, Z. Naturforsch. 51B (1996) 32–36.
[42] C. Cossy, A.C. Barnes, J.E. Enderby, A.E. Merbach, J. Chem. Phys. 90 (1989) 3254–3259.
[43] D.X. Jia, A.M. Zhu, J. Deng, Y. Zhang, J. Dai, Dalton Trans. (2007) 2083–2086.